THE ASTROPHYSICAL JOURNAL, 479:948–959, 1997 April 20

DISTANT COMPANIONS AND PLANETS AROUND MILLISECOND PULSARS

KRITEN J. JOSHI[1] AND FREDERIC A. RASIO[2,3]
Department of Physics, Massachusetts Institute of Technology
Received 1996 August 2; accepted 1996 November 13

ABSTRACT

We present a general method for determining the masses and orbital parameters of binary millisecond pulsars with long orbital periods ($P_{\rm orb} \gg 1$ yr), using timing data in the form of pulse frequency derivatives. Our method can be used even when the available timing data cover only a small fraction of an orbit, but it requires high-precision measurements of up to five successive derivatives of the pulse frequency. With five derivatives a complete determination of the mass and orbital parameters is in principle possible (up to the usual inclination factor $\sin i$). With less than five derivatives, only partial information can be obtained, but significant constraints can sometimes be placed on, e.g., the mass of the companion. We apply our method to analyze the properties of the second companion in the PSR B1620−26 triple system. We use the latest timing data for this system, including a recent detection of the fourth time derivative of the pulse frequency, to constrain the mass and orbital parameters of the second companion. We find that all possible solutions have a mass m_2 in the range $2.4 \times 10^{-4}\ M_\odot \leq m_2 \sin i_2 \leq 1.2 \times 10^{-2}\ M_\odot$, i.e., almost certainly excluding a second companion of stellar mass and suggesting instead that the system contains a planet or brown dwarf. To further constrain this system, we have used preliminary measurements of the secular perturbations of the inner binary. Using Monte Carlo realizations of the triple configuration in three dimensions, we find the most probable value of m_2 to be $0.01 \pm 0.005\ M_\odot$, corresponding to a distance of 38 ± 6 AU from the center of mass of the inner binary (the errors indicate 80% confidence intervals). We also apply our method to analyze the planetary system around PSR B1257+12, where a distant, giant planet may be present in addition to the three well-established Earth-mass planets. We find that the simplest interpretation of the frequency derivatives implies the presence of a fourth planet with a mass of $\sim 100\ M_\oplus$ in a circular orbit of radius ~ 40 AU.

Subject headings: celestial mechanics, stellar dynamics — planetary systems — pulsars: general — pulsars: individual (PSR B1620−26, PSR B1257+12)

1. INTRODUCTION

The traditional method for obtaining masses and orbital parameters of binary pulsars consists of fitting Keplerian or post-Newtonian models to timing data covering at least one complete orbit. For wide-orbit binary pulsars, with orbital periods longer than a few years to decades, fitting a complete orbit may not be possible. For such systems, we present a method for obtaining the masses and orbital parameters by using measured values of the successive time derivatives of the pulse frequency ($\dot{f}, \ddot{f}, f^{(3)}$, etc.). Given the high precision of millisecond pulsar timing, it is sometimes possible to measure these frequency derivatives up to high order with only a few years of observations. We show below that with *five derivatives* a complete solution may be obtained, with the orbital parameters and companion mass fully determined up to the usual unknown inclination factor $\sin i$. This solution is constructed under the assumption that all frequency derivatives are *dynamically induced* rather than being intrinsic to the pulsar spin-down. This is a crucial assumption and may not always be justified. Its validity, and the effects of relaxing it, must be examined for each particular application. If only three or four derivatives have been measured, significant constraints can still be placed on the parameters of the system. With just three dynamically induced derivatives and the assumption of a circular orbit (often justified, e.g., for a planet), a complete solution can again be obtained. Our method is not a substitute for the standard fitting procedure to data covering a complete orbit. Instead, it provides a way of obtaining the orbital parameters of wide-orbit binaries, which cannot be observed over a complete orbit because of their very long orbital periods. The method can only be successfully applied to binaries containing fast millisecond pulsars with low timing noise, in which one can reasonably expect the dynamically induced pulse frequency derivatives to dominate over intrinsic changes.

Applications of our method to two systems, PSR B1620−26 and PSR B1257+12, are presented in this paper. Both these systems are thought to contain planetary-mass companions to the millisecond pulsar (Wolszczan 1994; Arzoumanian et al. 1996). Their properties are of great interest for our understanding of planetary formation outside the solar system. This is particularly true in light of the many recent detections of extrasolar planets around nearby stars, which show a great diversity of properties (Mayor & Queloz 1995; Butler & Marcy 1996; Marcy & Butler 1996). PSR B1620−26, in the globular cluster M4, is in a hierarchical triple configuration. Previously available timing data allowed a second companion's mass anywhere in the range $\sim 10^{-3}$ to $\sim 1\ M_\odot$ (Michel 1994; Sigurdsson 1995), i.e., including the possibility of a Jupiter-type planet. PSR B1257+12 has three confirmed low-mass planets, and there is recent evidence for a fourth, more massive one (Wolszczan 1996).

Our paper is organized as follows: In § 2, we describe our general method for obtaining the companion mass and the orbital parameters by using measured pulse frequency

[1] Postal address: Mail Stop 6-218M, Massachusetts Institute of Technology, 77 Massachusetts Avenue, Cambridge, MA 02139; kjoshi@mit.edu.
[2] Postal address: Mail Stop 6-201, Massachusetts Institute of Technology, 77 Massachusetts Avenue, Cambridge, MA 02139; rasio@mit.edu.
[3] Alfred P. Sloan Foundation Fellow.

derivatives. In § 3, we apply our method to PSR B1620−26. We also incorporate into our analysis preliminary measurements of secular perturbations of the inner binary by performing Monte Carlo simulations with the undetermined parameters in the system to obtain the most probable mass for the second companion. In § 4, we apply our method to check whether the observed frequency derivatives of PSR 1257+12 are consistent with the possible existence of a fourth object in the planetary system.

2. INVERTING FREQUENCY-DERIVATIVE DATA

In the standard method for determining the parameters of binary pulsars, the data (consisting of radio pulse arrival times) are fitted to the predictions of a Keplerian or post-Newtonian model of the binary orbit. To obtain a reliable fit, one usually needs timing data covering at least a few complete orbital periods. However, even if the data do not cover a full period, it is still possible to determine, at least approximately, the companion's mass and the orbital parameters of the system if sufficiently accurate timing data are available. The method we develop here uses time derivatives of the pulse frequency (basically the coefficients in a Taylor expansion of the pulse frequency around a particular epoch). Pulse frequency derivatives are a convenient way in which radio astronomers can present the results of their observations when a clear periodicity cannot be recognized in the timing data.

2.1. *General Formulation*

Assuming that the pulsar's mass ($m_1 \simeq 1.4\,M_\odot$) is known, there are five parameters that can in principle be determined using our method: the mass of the companion m_2 (up to the unknown inclination angle i_2), the semimajor axis a_2, the eccentricity e_2, the longitude of pericenter ω_2 (measured from the ascending node), and the longitude λ_2 of the companion at the reference epoch (measured from pericenter). The inclination angle i_2 is the angle between the normal to the orbital plane and the line of sight; this angle cannot be determined directly from the timing data. Here and throughout this paper, a subscript "1" refers to the pulsar, a subscript "2" refers to the companion, and all orbital elements correspond to the motion around the center of mass of the system (e.g., the distance between the pulsar and its companion is $r_1 + r_2$).

If frequency derivatives up to the *fifth order* are measured, all five parameters (m_2, a_2, e_2, ω_2, λ_2) can in principle be determined. For small values of m_2/m_1, the usual combination $m_2 \sin i_2$ can be obtained (see the discussion for PSR B1620−26 in § 3). For larger companion masses, the dependence of the solutions on i_2 is more complicated, and one needs to adopt a particular value of $\sin i_2$ (in practice, $\sin i_2 \lesssim 1$ for a random orientation) in order to solve explicitly for m_2.

Our method assumes that the measured frequency derivatives are purely those induced by the motion of the pulsar (acceleration, jerk, and higher derivatives) around the binary's center of mass. This requires correcting the measurements for other possible kinematic effects (see, e.g., Camilo, Thorsett, & Kulkarni 1994). More importantly, one must assume that any intrinsic contribution from the pulsar spin-down can be neglected, or determined to some extent from the known properties of other millisecond pulsars and subtracted from the measured values. In particular, the observed first frequency derivative $\dot{f}$ is in general determined by a combination of acceleration and intrinsic spin-down of the pulsar,

$$\dot{f}_{\rm obs} = \dot{f}_{\rm int} + \dot{f}_{\rm acc} \,. \tag{1}$$

It is not possible to measure the two components separately in general. For some systems, however, it is reasonable to assume that $|\dot{f}_{\rm int}| \ll |\dot{f}_{\rm acc}|$ if $|\dot{f}_{\rm obs}|$ is large. For example, the observed $\dot{f}_{\rm obs}$ may be positive, a clear sign that it is determined predominantly by acceleration (as in the M15 pulsars PSR 2127+11A, D; Wolszczan et al. 1989). The expected value of $\dot{f}_{\rm int}$ may also be estimated from the pulse frequency f and from the assumption that the timing age $\tau \equiv \frac{1}{2} f/\dot{f}$ of a millisecond pulsar should satisfy $\tau \gtrsim 10^9$ yr. Indeed, most millisecond pulsars with reliably measured timing ages appear to satisfy this property (see, e.g., Phinney & Kulkarni 1994). Note that the true ages of some millisecond pulsars may be considerably smaller (cf. Lorimer et al. 1995), but this does not affect our argument. Similarly, the expected value of $\ddot{f}_{\rm int}$ can be estimated from the predicted level of *timing noise* for the pulsar, which, although very small for millisecond pulsars, may also affect the interpretation of $\ddot{f}_{\rm obs}$ (see, e.g., Arzoumanian et al. 1994; Kaspi, Taylor, & Ryba 1994). Intrinsic higher derivatives ($f^{(3)}$, etc.) are normally not measurable for millisecond pulsars, and therefore we can always assume safely that any measured values are dynamically induced.

After subtraction of known kinematic and intrinsic contributions, we can write the time derivatives of the pulse frequency at a particular reference epoch as

$$\dot{f} = -f\frac{\boldsymbol{a}\cdot\hat{\boldsymbol{n}}}{c}\,, \quad \ddot{f} = -f\frac{\dot{\boldsymbol{a}}\cdot\hat{\boldsymbol{n}}}{c} + \frac{\dot{f}^2}{f}\,, \quad \text{etc.}\,, \tag{2}$$

where c is the speed of light, $\boldsymbol{a}$ is the acceleration of the pulsar, and $\hat{\boldsymbol{n}}$ is a unit vector in the direction of the line of sight, and where an overdot indicates a time derivative. The second term in the expression for $\ddot{f}$ is smaller than the first by a factor $\sim v/c$, where v is the orbital velocity of the neutron star, i.e., $\dot{f}^2/f \ll |\ddot{f}|$. For $f^{(3)}$, we have $|\dot{f}\ddot{f}/f| \ll |f^{(3)}|$, etc., so that all similar terms can be neglected in taking higher and higher derivatives. Therefore we can write the first five frequency derivatives simply as

$$\begin{aligned} \dot{f} &= -f\frac{\boldsymbol{a}\cdot\hat{\boldsymbol{n}}}{c}\,, \\ \ddot{f} &= -f\frac{\dot{\boldsymbol{a}}\cdot\hat{\boldsymbol{n}}}{c}\,, \\ &\vdots \\ f^{(5)} &= -f\frac{\boldsymbol{a}^{(4)}\cdot\hat{\boldsymbol{n}}}{c}\,. \end{aligned} \tag{3}$$

Equation (3) forms a system of five nonlinear algebraic equations with five unknowns (m_2, a_2, e_2, λ_2, and ω_2), which must be solved numerically. It is straightforward but tedious to write down explicitly the right-hand sides of these equations in terms of the five unknowns, and we will omit their explicit forms in the general case. Some of the steps involved, however, are described below in § 2.2.

2.2. *Solution with Four Derivatives*

When four derivatives ($\dot{f}$ through $f^{(4)}$) are known, one can obtain a one-parameter family of solutions. In practice,

the problem can be reduced to solving a system of *three* nonlinear equations as follows: If m_1 is the mass of the pulsar and m_2 is the mass of the companion, the acceleration of the pulsar in its motion around the center of mass of the binary is of magnitude $a = k/r_1^2$, where r_1 is the distance from the pulsar to the center of mass and where

$$k = G\frac{m_2^3}{(m_1 + m_2)^2}. \tag{4}$$

For an elliptic Keplerian orbit of semimajor axis a_1 and eccentricity $e_1 = e_2$, the distance r_1 is given by

$$\frac{1}{r_1} = \frac{1}{h}(1 + e_2 \cos \lambda_1) \equiv \frac{A}{h}, \tag{5}$$

where $h = a_1(1 - e_2^2)$. Equation (3) for the pulse frequency derivatives can then be written

$$\dot{f} = -f\frac{a}{c}\sin(\lambda_1 + \omega_1)\sin i_2 = -fKA^2 \sin(\lambda_1 + \omega_1), \tag{6}$$

$$\ddot{f} = -fKB\dot{\lambda}_1, \tag{7}$$

$$f^{(3)} = -fKC\dot{\lambda}_1^2, \tag{8}$$

$$f^{(4)} = -fKD\dot{\lambda}_1^3, \tag{9}$$

where we have defined

$$A = 1 + e_2 \cos \lambda_1,$$

$$B = 2AA' \sin(\lambda_1 + \omega_1) + A^2 \cos(\lambda_1 + \omega_1),$$

$$C = B' + \frac{2BA'}{A}, \quad D = C' + \frac{4CA'}{A},$$

$$K = \frac{k \sin i_2}{h^2 c}, \tag{10}$$

with a prime indicating a derivative with respect to λ_1.

Using equation (6), we can rewrite equations (7)–(9) as

$$\ddot{f} = \frac{B\dot{\lambda}_1 \dot{f}}{A^2 \sin(\lambda_1 + \omega_1)}, \tag{11}$$

$$f^{(3)} = \frac{C\dot{\lambda}_1^2 \dot{f}}{A^2 \sin(\lambda_1 + \omega_1)}, \tag{12}$$

$$f^{(4)} = \frac{D\dot{\lambda}_1^3 \dot{f}}{A^2 \sin(\lambda_1 + \omega_1)}. \tag{13}$$

This is a nonlinear system of three equations with four unknowns—e_2, $\lambda_1 = \lambda_2$, $\omega_1 = \omega_2 + 180°$, and $\dot{\lambda}_1$. Assuming a value for one of them, we can solve for the remaining parameters.

We have chosen to use the eccentricity e_2 as our free parameter. For an assumed value of e_2, we solve equations (11)–(13) for λ_1, $\dot{\lambda}_1$, and ω_1 using the Newton-Raphson method (see, e.g., Press et al. 1992). This method requires an initial guess for the unknown parameters, which is then successively improved until convergence to an actual solution is obtained. One must be careful to experiment with many different initial guesses since nonlinear systems like this often have multiple branches of solutions. In addition, symmetries must also be taken into account. Here physically equivalent solutions are obtained if the direction of motion is reversed, and the signs of ω_1 and λ_1 are also reversed. This gives a different but equivalent orientation of the system. Once λ_1, $\dot{\lambda}_1$, and ω_1 are known, conservation of angular momentum, together with equation (6), yields

$$\frac{k}{h^3} = \frac{\dot{\lambda}_1^2}{A^4}, \tag{14}$$

$$\frac{k}{h^2} = -\frac{\dot{f}c}{fA^2 \sin(\lambda_1 + \omega_1)\sin i_2}. \tag{15}$$

Using equations (14) and (15), we can calculate k and h:

$$h = -\frac{\dot{f}cA^2}{f \sin i_2 \sin \lambda_1 \dot{\lambda}_1^2}, \tag{16}$$

$$k = -\left(\frac{\dot{f}c}{f \sin i_2 \sin \lambda_1}\right)^3 \left(\frac{A^2}{\dot{\lambda}_1^4}\right). \tag{17}$$

It is now straightforward to obtain m_2 (from k, assuming that the pulsar mass m_1 is known) and the semimajor axis $a_2 = (m_1/m_2)h/(1 - e_2^2)$. When $m_2 \ll m_1$, we can directly obtain $m_2 \sin i_2$ as follows: For small m_2, we have $k \approx Gm_2^3/m_1^2$. Therefore $m_2 \approx (km_1^2/G)^{1/3}$ and equation (17) yields

$$m_2 \sin i_2 \approx \frac{\dot{f}c}{f \sin \lambda_1}\left(\frac{m_1^2 A^2}{G\dot{\lambda}_1^4}\right)^{1/3}. \tag{18}$$

For larger values of m_2/m_1, one needs to assume a value for $\sin i_2$ and solve equation (4) numerically for m_2.

2.3. *Solution with Three Derivatives*

When only three derivatives are known, one can assume values for two parameters and solve for the remaining three parameters in the same way as above. Alternatively, in the special case of a circular orbit ($e_2 = 0$), the system can be solved completely (to within $\sin i_2$) by using only three derivatives. In that case, we have

$$\dot{f} = \frac{-fk \sin i_2}{a_1^2 c} \sin \lambda_1, \tag{19}$$

$$\ddot{f} = \frac{-fk \sin i_2}{a_1^2 c}(\cos \lambda_1)\dot{\lambda}_1, \tag{20}$$

$$f^{(3)} = \frac{fk \sin i_2}{a_1^2 c}(\sin \lambda_1)\dot{\lambda}_1^2. \tag{21}$$

Note that here λ_1 is the longitude of the pulsar *measured from the ascending node* (*not* from pericenter, as before).

Using equation (19) to eliminate $-fk \sin i_2/a_1^2 c$, we obtain

$$\ddot{f} = \frac{\dot{f}}{\sin \lambda_1}(\cos \lambda_1)\dot{\lambda}_1, \tag{22}$$

$$f^{(3)} = -\dot{f}\dot{\lambda}_1^2. \tag{23}$$

This yields

$$\dot{\lambda}_1^2 = -f^{(3)}/\dot{f}, \tag{24}$$

$$\lambda_1 = \arctan\left[\frac{\dot{f}}{\ddot{f}}\left(\frac{-f^{(3)}}{\dot{f}}\right)^{1/2}\right]. \tag{25}$$

Using equation (19) and conservation of angular momentum, we have

$$\frac{k}{a_1^2} = \frac{-\dot{f}c}{f \sin i_2 \sin \lambda_1}, \tag{26}$$

$$\frac{k}{a_1^3} = \dot{\lambda}_1^2 . \tag{27}$$

Dividing equation (26) by equation (27) and then using equations (24), (25), and (27), we obtain

$$a_1 = \frac{\dot{f}^2 c}{f f^{(3)} \sin i_2 \sin \lambda_1}, \tag{28}$$

$$k = -\left(\frac{\dot{f}c}{f \sin i_2 \sin \lambda_1}\right)^3 \left(\frac{\dot{f}}{f^{(3)}}\right)^2 , \tag{29}$$

where λ_1 is given by equation (25). For $m_2 \ll m_1$, we have $k \approx Gm_2^3/m_1^2$. Then, for given values of the frequency derivatives and the pulsar mass m_1, the companion mass m_2 can be calculated explicitly by using equation (29). We find

$$m_2 \sin i_2 \approx -\left(\frac{m_1^2}{G}\right)^{1/3} \left(\frac{\dot{f}c}{f \sin \lambda_1}\right) \left(\frac{\dot{f}}{f^{(3)}}\right)^{2/3} , \tag{30}$$

where λ_1 is given by equation (25). Finally, we can calculate $a_2 = (m_1/m_2)a_1$, where a_1 is given by equation (28).

2.4. *Solution with Two Derivatives*

When only two derivatives are available, one can obtain a one-parameter family of solutions, assuming again that $e_2 \approx 0$. We can use $f^{(3)}$ (or, equivalently, $\dot{\lambda}_1$, using eq. [24]) as the free parameter and then use the equations of § 2.3 to construct a one-parameter family of solutions explicitly.

3. APPLICATION TO THE PSR B1620−26 TRIPLE SYSTEM

The millisecond pulsar PSR B1620−26, in the globular cluster M4, has a low-mass binary companion (probably a white dwarf of mass $m_c \approx 0.3\ M_\odot$ for a pulsar mass $m_p = 1.35\ M_\odot$) in a 191 day low-eccentricity orbit (Lyne et al. 1988; McKenna & Lyne 1988). The unusually large second and third frequency derivatives indicate the presence of a *second companion* around the inner binary, forming a hierarchical triple configuration (Backer 1993; Backer, Foster, & Sallmen 1993; Thorsett, Arzoumanian, & Taylor 1993). Such hierarchical triple systems are expected to be produced quite easily in dense globular clusters through dynamical interactions between binaries. In a typical interaction, one star would be ejected, leaving the other three in a stable triple system (Rasio, McMillan, & Hut 1995; Sigurdsson 1995). Previous calculations (performed using frequency derivatives up to the third order) have shown that the mass of the second companion could be anywhere from $\sim 10^{-3}$ to $\sim 1\ M_\odot$ (Michel 1994; Sigurdsson 1995). Recently, a measurement was made of the fourth derivative of the pulse frequency, along with preliminary measurements of secular changes of the inner binary parameters due to the perturbation of the second companion (Arzoumanian et al. 1996). These include a precession of the inner binary orbital plane (measured as a change in the projected semimajor axis of the binary) and possible changes in the eccentricity and longitude of periastron.

3.1. *Modeling the Frequency Derivatives*

In this section, we apply the method described in § 2.2 to analyze the properties of the second companion in the PSR B1620−26 triple system. Since the orbital period of the second companion is much longer than that of the inner binary (for all solutions obtained below), we treat the inner binary as a single object. Keeping the same notation as before, we let $m_1 = m_p + m_c$ be the mass of the inner binary pulsar, with m_p the mass of the neutron star and m_c the mass of the (inner) companion, and we denote by m_2 the mass of the second companion (to be determined). As in § 2, the orbital parameters (λ_2, ω_2, e_2, a_2, and i_2) refer to the orbit of the (second) companion with respect to the center of mass of the system (here the entire triple). However, a subscript "1" for the orbital elements refers to the orbit of the inner binary. The results presented in this section are all for $m_1 = 1.7\ M_\odot$ (assuming $m_p = 1.4\ M_\odot$ and $m_c = 0.3\ M_\odot$; cf. Thorsett et al. 1993). However, we have checked that they are not very sensitive to small changes in the value of m_1. In particular, the companion mass m_2 varies only as $\sim m_1^{2/3}$ (see eq. [4]).

We use the latest available values of the pulse frequency derivatives (Arzoumanian & Thorsett 1997) for the epoch MJD 48,725.0:

$$\begin{aligned} f &= 90.2873320054(1)\ \mathrm{s}^{-1} , \\ \dot{f} &= -5.4702(7) \times 10^{-15}\ \mathrm{s}^{-2} , \\ \ddot{f} &= 1.929(8) \times 10^{-23}\ \mathrm{s}^{-3} , \\ f^{(3)} &= 8(1) \times 10^{-33}\ \mathrm{s}^{-4} , \\ f^{(4)} &= -2.1(6) \times 10^{-40}\ \mathrm{s}^{-5} . \end{aligned} \tag{31}$$

These values take into account a (very precise) Keplerian model of the inner orbit. The corrections to $\dot{f}$ due to proper motion are negligible for this pulsar. The frequency derivatives should therefore reflect the residual motion of the pulsar caused by the presence (unmodeled) of a second companion. However, as discussed in § 2.1, the observed first derivative $\dot{f}_{\rm obs}$ can be a combination of the intrinsic spin-down of the pulsar and the acceleration due to the second companion. Since $\dot{f}_{\rm obs}$ is negative and $\dot{f}_{\rm int}$ is always negative, $\dot{f}_{\rm acc}$ can in principle be either positive or negative. If it is negative, then its magnitude must be $\leq |\dot{f}_{\rm obs}|$. If it is positive, its magnitude can in principle be larger. However, it cannot be much larger than $|\dot{f}_{\rm obs}|$ since this would imply a very large intrinsic spin-down rate and a short characteristic age $\tau = -\frac{1}{2} f/\dot{f}$, which is not expected for a millisecond pulsar (cf. Thorsett et al. 1993 and § 2.1). In practice, we find that varying $\dot{f}_{\rm acc}/\dot{f}_{\rm obs}$ in the entire range -1.0 to $+1.0$ does not affect our solutions significantly (see below). The expected value of $\ddot{f}$ due to timing noise can be estimated using, e.g., Figure 1 of Arzoumanian et al. (1994), which gives the timing noise parameter $\Delta_8 \equiv \log (|\ddot{f}|\, 10^{24}/6f)$ as a function of period derivative. This yields an *upper limit* on the contribution to $\ddot{f}$ due to intrinsic timing noise of $3 \times 10^{-24}\ \mathrm{s}^{-3}$, which is an order of magnitude smaller than $|\ddot{f}_{\rm obs}|$. The same conclusion is reached if we consider, for comparison, PSR B1855+09, which has a comparable spin rate ($f = 186\ \mathrm{s}^{-1}$) but a frequency second derivative $|\ddot{f}_{\rm obs}| \leq 2 \times 10^{-27}\ \mathrm{s}^{-3}$ (3 σ), i.e., at least 4 orders of magnitude smaller than $\ddot{f}_{\rm obs}$ in PSR B1620−26 (Kaspi et al. 1994).

Figure 1 illustrates our "standard solution," obtained under the assumption that $\dot{f}_{\rm acc} = \dot{f}_{\rm obs}$ and using the current best-fit value for the fourth derivative, $f_m^{(4)} = -2.1 \times 10^{-40}\ \mathrm{s}^{-5}$. Following the method of § 2.2, we use e_2 as

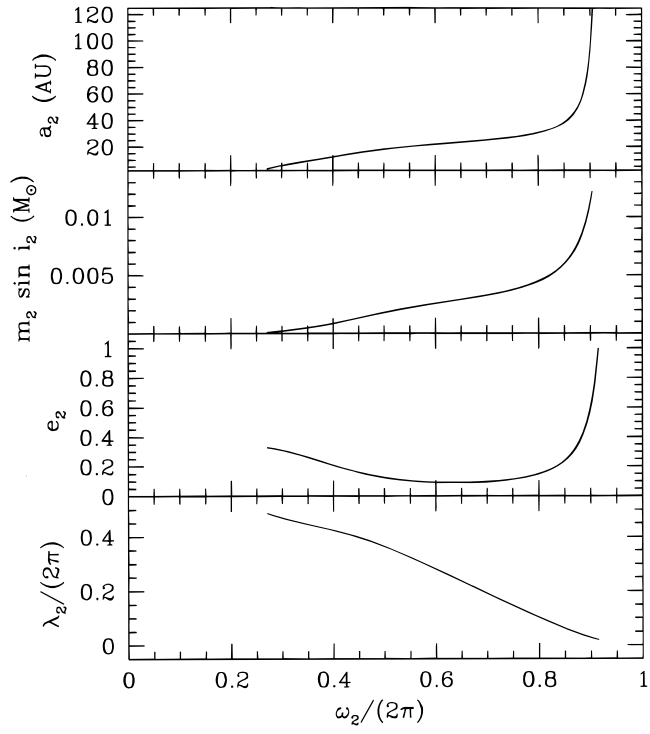

FIG. 1.—Allowed values of the semimajor axis a_2, mass m_2, eccentricity e_2, longitude at epoch λ_2, and longitude of pericenter ω_2 for the second companion of PSR B1620−26, using the latest available values for all pulse frequency derivatives. This is our "standard solution," using the present best-fit value $f_m^{(4)} = -2.1 \times 10^{-40}$ s^{-5} and assuming that all measured frequency derivatives are dynamically induced. Acceptable solutions all have $2.4 \times 10^{-4}\, M_\odot \le m_2 \sin i_2 \le 1.2 \times 10^{-2}\, M_\odot$.

the free parameter. We see that there are no solutions for $e_2 \lesssim 0.1$. Hence a nearly circular orbit is ruled out. For $0.1 \lesssim e_2 \lesssim 0.3$, there are two solutions for each value of the eccentricity and hence two possible values of m_2.

In the first branch of solutions, m_2 approaches zero as the eccentricity approaches the value $e_2 \approx 0.33$. However, for very small m_2, the second companion gets close enough to the inner binary to make the triple configuration dynamically unstable. The stability of the triple system can be checked by using an approximate criterion of the form $Y \ge Y_{\rm min}$ (for stability), where $Y = [(1 - e_2)(a_1 + a_2)]/[(a_p + a_c)(1 + e_1)]$ is the ratio of the outer pericenter separation (from the center of mass of the inner binary to the second companion) to the apastron separation of the inner binary. Here we have used the results of Eggleton & Kiseleva (1995), who give

$$Y_{\rm min} \approx 1 + \frac{3.7}{q_{\rm out}^{1/3}} + \frac{2.2}{1 + q_{\rm out}^{1/3}} + \frac{1.4}{q_{\rm in}^{1/3}} \frac{q_{\rm out}^{1/3} - 1}{q_{\rm out}^{1/3} + 1}. \quad (32)$$

Here $q_{\rm in} = m_p/m_c$ and $q_{\rm out} = m_1/m_2$ are the inner and outer mass ratios. Using the values $m_p \approx 1.4\, M_\odot$, $m_c \approx 0.3\, M_\odot$, and $m_2 \sim 10^{-5}\, M_\odot$, we obtain $Y_{\rm min} \approx 2$. Thus we require $Y \ge 2$ for a dynamically stable solution. This gives us a lower limit on the second companion's mass of $m_2 \gtrsim 3 \times 10^{-5}\, M_\odot \approx 10\, M_\oplus$. In addition, we can rule out solutions with orbital periods $P_2 \lesssim 14$ yr since this would have been detected already in the timing residuals (S. E. Thorsett 1996, private communication). This gives us a somewhat stricter lower limit of $m_2 \gtrsim 2.4 \times 10^{-4}\, M_\odot \approx 80\, M_\oplus$.

For the second branch of solutions, m_2 increases monotonically from $\sim 10^{-3}$ to $1.2 \times 10^{-2}\, M_\odot$ (i.e., from Jupiter to brown dwarf masses) as e_2 increases from ~ 0.1 to 1. As e_2 approaches 1.0, the mass m_2 remains bound. So even though the solutions with $e_2 \to 1$ are a priori unlikely, they provide a strict upper limit, $m_2 \le 1.2 \times 10^{-2}\, M_\odot$. Since all our solutions have $m_2 \ll m_1$, our method in fact yields the product $m_2 \sin i_2$ (cf. § 2.2), which we show in Figure 1.

The effect of varying $\dot f_{\rm acc}/\dot f_{\rm obs}$ in the range 0–1.0 is shown in Figure 2. We see that smaller values of $\dot f_{\rm acc}/\dot f_{\rm obs}$ yield slightly solutions with smaller mass, but the overall mass range is not significantly affected. In particular, we see that stellar-mass solutions for m_2 are not allowed even if the observed value of $\dot f$ is assumed to be mostly intrinsic. Negative values of $\dot f_{\rm acc}/\dot f_{\rm obs}$ yield similar results.

We see that our standard solution excludes the stellar mass range ($m_2 \gtrsim 0.1\, M_\odot$) for the second companion, and this is rather surprising. A stellar mass would provide a natural explanation for the anomalously high eccentricity of the inner binary ($e_1 \approx 0.03$) in terms of secular perturbations (Rasio 1994). In addition, a stellar mass would also be consistent with a preliminary identification of an optical counterpart for the system (Bailyn et al. 1994). We have seen already that assuming a different value for $\dot f_{\rm acc}$ does not change our conclusions. Alternatively, we can try to vary the value of $f^{(4)}$ within its fairly large error bar. However, we find that varying $f^{(4)}$ within its formal 1 σ error bar still does not produce significant changes in m_2. In order to obtain stellar-mass solutions, we find that we must vary $f^{(4)}$ within a larger 4 σ error bar around the best-fit value $f_m^{(4)}$ given above. Note that this allows for a change of sign in the

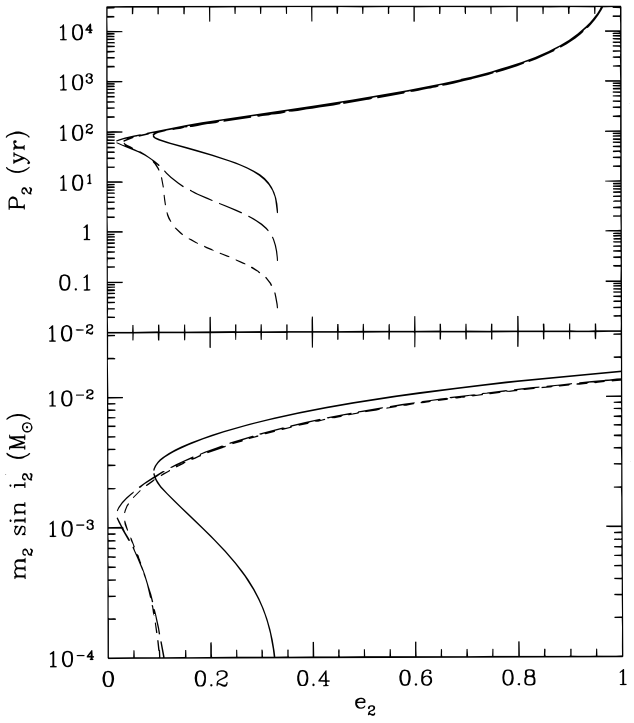

FIG. 2.—Orbital period, mass, and eccentricity of the second companion of PSR B1620−26 for different values of the acceleration-induced first frequency derivative. The curves are for $\dot f_{\rm acc} = \dot f_{\rm obs}$ (*solid line*), $\dot f_{\rm acc} = 0.1 \dot f_{\rm obs}$ (*long-dashed line*), and $\dot f_{\rm acc} = 0.01 \dot f_{\rm obs}$ (*short-dashed line*). We assume that the inclination angle $i_2 = 90°$. We see that the mass range does not change significantly when varying $\dot f_{\rm acc}$ and that stellar masses are always excluded.

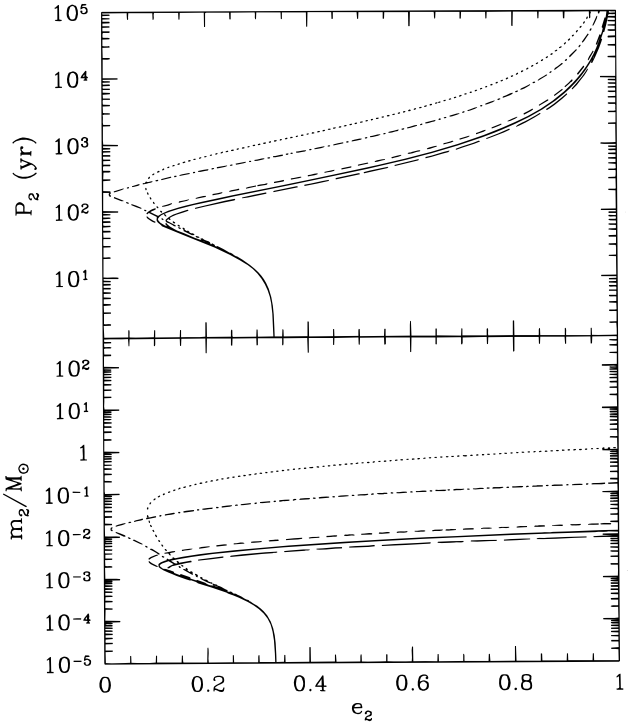

FIG. 3.—Similar to Fig. 2, but the dependence of the solutions on $f^{(4)}$ is illustrated for an expanded 4 σ error bar around the best-fit value $f_m^{(4)} = -2.1 \times 10^{-40}$ s^{-5}. The solutions are shown for $f^{(4)} = f_m^{(4)}$ (*solid line*), $f^{(4)} = f_m^{(4)} - (1\ \sigma)$ (*long-dashed line*), $f^{(4)} = f_m^{(4)} + (1\ \sigma)$ (*short-dashed line*), $f^{(4)} = 0.1 f_m^{(4)}$ (*dot-dashed line*), and $f^{(4)} = 0.01 f_m^{(4)}$ (*dotted line*), where $\sigma = 0.6 \times 10^{-40}$ s^{-5}. Stellar-mass solutions are obtained when $-0.1 \lesssim f^{(4)}/f_m^{(4)} \lesssim 0.1$.

actual value of $f^{(4)}$. The results are illustrated in Figure 3. Here we assume that $\sin i_2 = 1$. We find that stellar-mass solutions (with $m_2 \gtrsim 0.1\ M_\odot$) are possible only if $-0.1 \lesssim f^{(4)}/f_m^{(4)} \lesssim 0.1$; i.e., $f^{(4)}$ must be more than 3 σ away from its present best-fit value (assuming that $\sin i_2 \approx 1$).

3.2. *Secular Perturbations of the Inner Binary*

We can further constrain the system by considering secular perturbations in the orbital elements of the inner binary. Preliminary measurements have been made of the perturbations in ω_1, e_1, and x_1 (Arzoumanian et al. 1996; Arzoumanian & Thorsett 1997). We use these measurements to further constrain the system by requiring that all our solutions be consistent with these secular perturbations.

Since the period P_2 of the second companion is much larger than the period of the inner binary, we can calculate the secular perturbations by assuming that the second companion has a fixed position in space with respect to the inner binary. Let r_{12}, θ_2, and ϕ_2 be the fixed spherical polar coordinates of the second companion, with the origin at the center of mass of the inner binary, ϕ_2 measured from pericenter in the orbital plane, and θ_2 such that $\sin \theta_2 = 1$ for the coplanar case. Then the averaged perturbation rates are given by

$$\dot{\omega}_1 = \frac{3\pi\eta}{P_1} [\sin^2 \theta_2 (5 \cos^2 \phi_2 - 1) - 1] , \tag{33}$$

$$\dot{e}_1 = \frac{-15\pi}{2P_1} \eta e_1 \sin^2 \theta_2 \sin 2\phi_2 , \tag{34}$$

$$\dot{i}_1 = \frac{3\pi}{2P_1} \eta \sin 2\theta_2 \cos (\omega_1 + \phi_2) \tag{35}$$

(Rasio 1994), where $P_1 = 16{,}540{,}653$ s is the period of the inner binary, $\eta = (m_2/m_1)[(a_p + a_c)/r_{12}]^3$, a_c is the semimajor axis of the inner binary companion, and a_p is the semimajor axis of the pulsar (with respect to the center of mass of the inner binary). The projected semimajor axis of the pulsar is $x_p = (1/c) a_p \sin i_1$, and therefore

$$\dot{x}_p = \frac{1}{c} a_p \cos i_1 \dot{i}_1 . \tag{36}$$

Note that there is no secular perturbation of the semimajor axis ($\dot{a}_p = 0$).

The present measured values of the perturbations are

$$\dot{\omega}_1 = (-2.0 \pm 2.1) \times 10^{-4} \text{ deg yr}^{-1} , \tag{37}$$

$$\dot{e}_1 = (5 \pm 3) \times 10^{-15} \text{ s}^{-1} , \tag{38}$$

$$\dot{x}_p = (-6.5 \pm 0.8) \times 10^{-13} \tag{39}$$

(Arzoumanian & Thorsett 1997). Only $\dot{x}_p$ is clearly detected, while the two others are at best marginal detections. Note that proper motion can also lead to a change in the projected semimajor axis x_p of the pulsar. However, if the observed $\dot{x}_p$ was due to proper motion, Arzoumanian et al. (1996) find that the inner binary companion of the pulsar would then have a mass $m_c > 1.0\ M_\odot$, with $i_1 < 10°$ for a 1.35 $M_\odot$ pulsar, which seems very unlikely. Hence we assume here that the observed $\dot{x}_p$ is caused by the secular precession of the inner orbit induced by the presence of the second companion.

To incorporate these measurements into our theoretical model, we have performed Monte Carlo simulations with the unknown variables in the system, namely, i_1, i_2, e_2, θ_2, and ϕ_2. The angles θ_2 and ϕ_2 can be determined by using i_1, i_2, ω_2, λ_2, and an additional undetermined angle α, which (along with i_1 and i_2) describes the relative orientation of the planes of the orbit of the inner binary and the orbit of the second companion. For a detailed description of the geometry, see the Appendix. We assume a uniform probability distribution for $\cos i_1$, $\cos i_2$, and α. Although there is no reason to expect the triple system to be in thermal equilibrium with the cluster (since the lifetime of the triple system in the core of M4 is only $\sim 10^7$ yr; see discussion in § 3.3), we assume a thermal distribution for e_2, i.e., a linear probability distribution Prob $(e_2) = 2e_2$ (see, e.g., Heggie 1975), for lack of a better alternative. Our procedure for constructing random realizations of the system is as follows: We start by assuming a value of e_2 and solving the nonlinear system numerically for m_2, a_2, λ_2, and ω_2 as described in § 3.1. Using this solution, we calculate $\eta = (m_2/m_1)[(a_p + a_c)/r_{12}]^3$. Then, for each trial, we generate random values for i_1, i_2, and α and calculate θ_2 and ϕ_2 as described in the Appendix. We choose the number of trials for each assumed value of e_2 so as to obtain a linear distribution for e_2 over all the trials. We then calculate the secular perturbation rates using equations (33)–(36), and we check for consistency with the observed values of the perturbations. We use a simple rejection algorithm, accepting

or rejecting a trial configuration based on a three-dimensional Gaussian probability distribution that is the product of Gaussian distributions for $\dot{\omega}_1$, $\dot{e}_1$, and $\dot{x}_p$ centered around their mean values and with standard deviations equal to the error bars given above.

In Figures 4 and 5, we show histograms of the number of successful trials for different values of m_2 and the corresponding distance r_{12} of the second companion from the inner binary, for both $f^{(4)} = f_m^{(4)}$ (standard solutions) and $f^{(4)} = 0.01 f_m^{(4)}$ (required to obtain stellar-mass solutions). For our standard solutions, we find that the mass distribution for the second companion peaks at $m_2 = 0.01 \pm 0.005$ $M_\odot$, corresponding to a distance of $r_{12} = 38 \pm 6$ AU. Note that this is the distance of the second companion from the binary (*not* the semimajor axis of the second companion).

Here the errors represent 80% confidence intervals. The semimajor axis a_2 and period P_2 are not well constrained and vary over 3 orders of magnitude. The period P_2 varies from about 10^2 to 10^4 yr with the distribution centered around 400 yr, and a_2 varies from about 10 to 1000 AU with the distribution centered around 70 AU. In the second case, the distribution peaks at $m_2 = 1.0 \pm 0.5$ $M_\odot$, corresponding to a distance of $r_{12} = 150 \pm 35$ AU. The period P_2 varies from about 10^3 to 10^5 yr with the distribution centered around 3000 yr, and a_2 varies from about 10^2 to 10^4 AU with the distribution centered around 200 AU. We obtain peaks in the stellar mass range for m_2 only when $-0.1 \lesssim f^{(4)}/f_m^{(4)} \lesssim 0.1$. In all cases, we find that the orientation of the second companion with respect to the inner binary (angles θ_2 and ϕ_2) is poorly constrained by the current data, as is the inclination i_2 of the second companion. The inclination of the binary is better constrained, to $\sim 55° \pm 15°$ (cf. Fig. 6). The eccentricity of the second companion, e_2, is also poorly constrained.

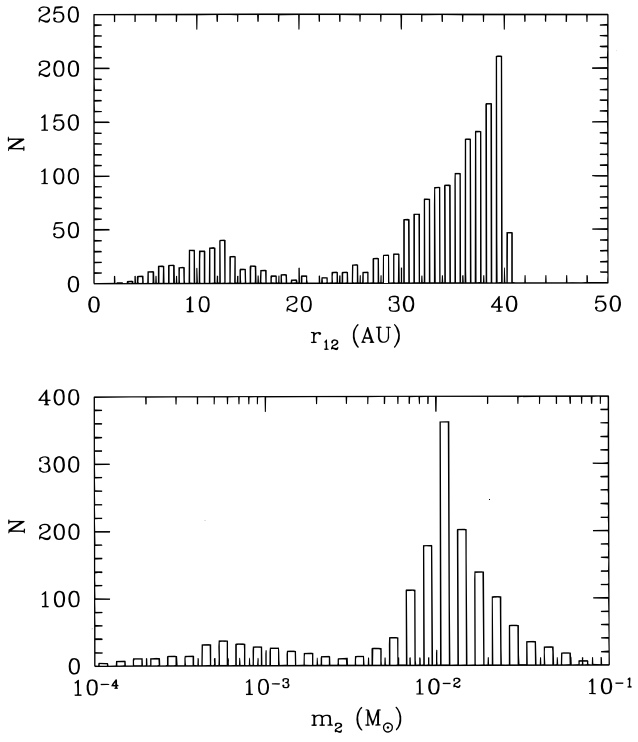

FIG. 4.—Histogram of the number of successful trials (N) for different values of m_2 and the corresponding distance r_{12} of the second companion from the inner binary for the case $f^{(4)} = f_m^{(4)}$ in our Monte Carlo simulations. We find that the most probable value for the second companion's mass is $m_2 = 0.01 \pm 0.005$ $M_\odot$, corresponding to a distance of $r_{12} = 38 \pm 6$ AU (80% confidence intervals).

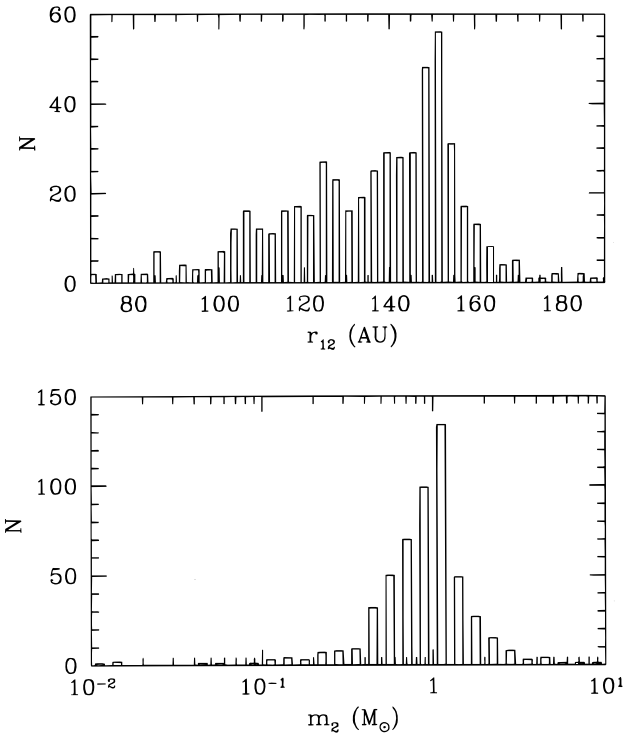

FIG. 5.—Same as Fig. 4, but for the case $f^{(4)} = 0.01 f_m^{(4)}$. We see that the most probable value for the second companion's mass is now $m_2 = 1.0 \pm 0.5$ $M_\odot$, corresponding to a distance of $r_{12} = 150 \pm 35$ AU.

3.3. *Model Predictions*

We can obtain a predicted value of the fifth pulse frequency derivative $f^{(5)}$ at the current epoch for each of our solutions by differentiating equation (9) for a specified value of e_2. In Figure 7, we show the most probable values for $f^{(5)}$ from the Monte Carlo simulations of § 3.2. For $f^{(4)} = f_m^{(4)}$ (standard solution), we find that the most probable value is $f^{(5)} = (0.15 \pm 0.05) \times 10^{-48}$ s^{-6} whereas, for $f^{(4)} = 0.01 f_m^{(4)}$ (which yields stellar-mass solutions), $f^{(5)} = (-6.0 \pm 0.4) \times 10^{-51}$ s^{-6}. Thus even a crude measurement of $f^{(5)}$ should completely settle the question of the second companion's mass.

We have also calculated the predicted evolution of the frequency derivatives $\dot{f}$ through $f^{(4)}$ for the next 20 years. We show the results for the typical orbit of a Jupiter- to brown dwarf–sized companion ($m_2 = 0.01$ $M_\odot$) in Figure 8 and for a stellar-mass companion ($m_2 = 0.5$ $M_\odot$) in Figure 9. In the first case, the orbit has $e_2 = 0.77$, a period $P_2 = 1562$ yr, and $a_2 = 160$ AU. We see that $\dot{f}$ changes sign in about 10 years and that $f^{(3)}$ decreases surprisingly rapidly, changing sign in about 1.5 years. For the stellar-mass case, only $\dot{f}$ changes sign within 10 years. The other frequency derivatives do not change significantly over 20 years. The orbit in this case has $e_2 = 0.49$, a period $P_2 = 2034$ yr, and $a_2 = 161$ AU. Thus a change in sign of $f^{(3)}$ within the next couple of years would provide additional support for the existence of a planet or brown dwarf in this system.

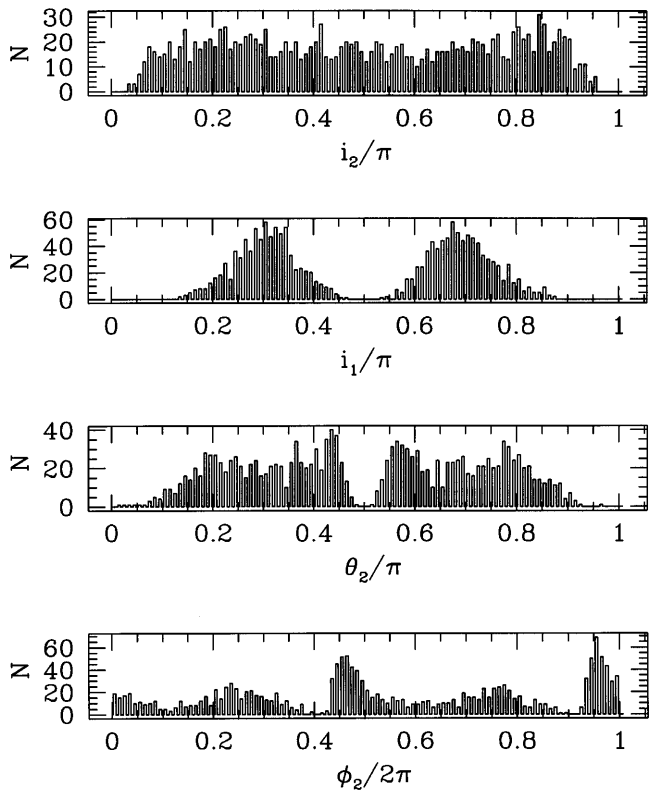

FIG. 6.—Histograms of the number of successful trials (N) for various parameters in the Monte Carlo simulations with $f^{(4)} = f_m^{(4)}$. All the angles are poorly constrained except the inclination of the inner binary, which is slightly better constrained to $i_1 \sim 55° \pm 15°$.

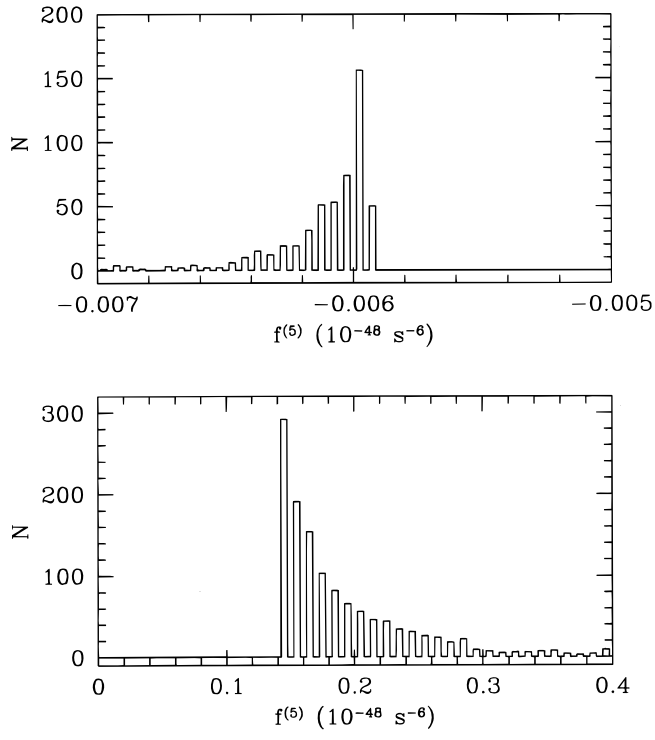

FIG. 7.—Most probable value of the fifth frequency derivative $f^{(5)}$ given by the Monte Carlo simulations. We obtain $f^{(5)} \approx 0.15(5) \times 10^{-48}$ s^{-6} for $f^{(4)} = f_m^{(4)}$ (*bottom*) and $f^{(5)} \approx -0.0060(4) \times 10^{-48}$ s^{-6} for $f^{(4)} = 0.01 f_m^{(4)}$ (*top*).

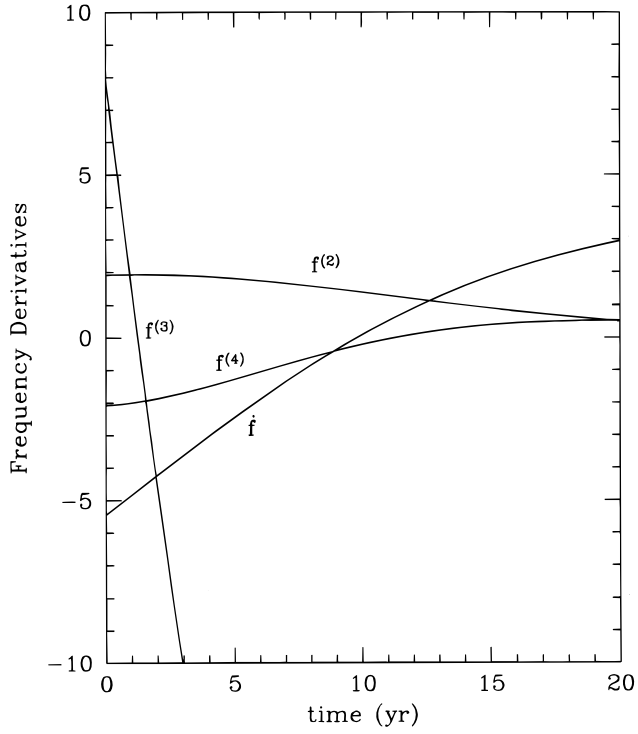

FIG. 8.—Predicted variation of the frequency derivatives over the next 20 yr for a low-mass ($m_2 = 0.01\ M_\odot$) second companion (standard solution). The units for the four derivatives are 10^{-15} s^{-2} for $\dot{f}$, 10^{-23} s^{-3} for $\ddot{f}$, 10^{-33} s^{-4} for $f^{(3)}$, and 10^{-40} s^{-5} for $f^{(4)}$. We see that $\dot{f}$ changes sign in ~ 10 yr, and $f^{(3)}$ changes sign in ~ 1.5 yr.

We also find that, in all cases, the values of $\ddot{f}$, $f^{(3)}$, and $f^{(4)}$ at *apastron* are at least 2, 3, and 5 orders of magnitude smaller, respectively, than their present observed values. This means that the triple nature of the system would probably remain undetectable near apastron. It is therefore reasonable to find the second companion relatively close to periastron in our solutions (within $\sim 15°$ for the case illustrated in Fig. 8 and $\sim 40°$ for the case considered in Fig. 9).

3.4. *Discussion*

As mentioned previously, the method for determining the orbital parameters of a binary pulsar presented in § 2, although quite general in its formulation, can only be applied successfully to systems containing fast millisecond pulsars, in which the dynamically induced frequency derivatives dominate the measurements. In addition, it requires several successively higher order frequency derivatives to be measured accurately. The PSR B1620−26 triple system satisfies all of these conditions and hence is ideally suited for analysis using our method. PSR B1620−26 has been observed for more than 7 years, and its hierarchical triple structure is strongly supported by all current observations (Backer et al. 1993; Thorsett et al. 1993; Arzoumanian & Thorsett 1997). The error bar on $f^{(4)}$ is likely to shrink rapidly as more timing data become available. If the actual value of $f^{(4)}$ is close to the current best-fit value $f_m^{(4)} = -2.1 \times 10^{-40}$ s^{-5}, then the second companion must have a mass $m_2 \leq 0.1\ M_\odot$ as long as the system has an inclination $i_2 \geq 7°$, with the most probable mass (given by our Monte Carlo simulations) being $0.01 \pm 0.005\ M_\odot$ (the error bar indicates an 80% confidence interval). If $f^{(4)}$ is within 1 σ of $f_m^{(4)}$, then the same result holds to within a factor of 2. A rather low

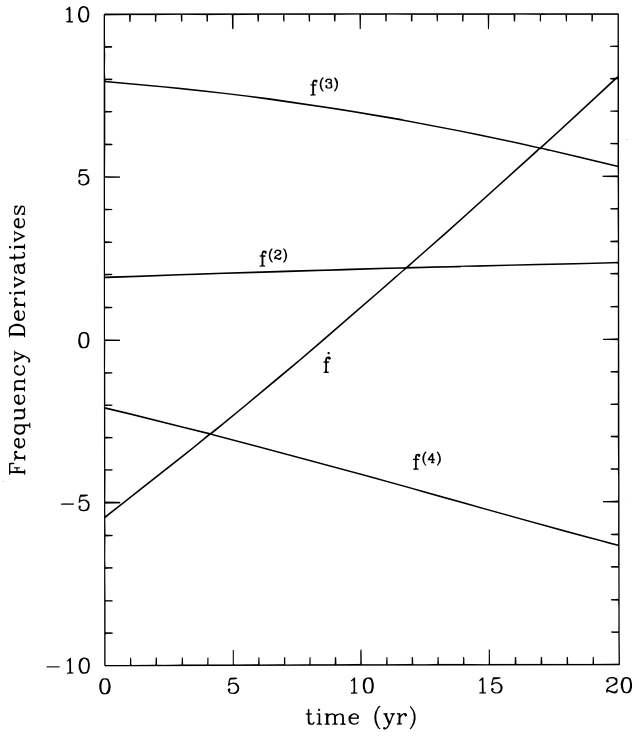

FIG. 9.—Predicted variation of the frequency derivatives over the next 20 yr for a stellar-mass ($m_2 = 0.5\ M_\odot$) second companion (assuming $f^{(4)} = 0.01 f_m^{(4)}$). The units for the four derivatives are 10^{-15} s^{-2} for $\dot{f}$, 10^{-23} s^{-3} for $\ddot{f}$, 10^{-33} s^{-4} for $f^{(3)}$, and 10^{-42} s^{-5} for $f^{(4)}$. We see that $\dot{f}$ changes sign in ~ 10 yr, but the other derivatives do not change much in 20 yr.

inclination angle ($i_2 \leq 10°$) or $|f^{(4)}/f_m^{(4)}| \leq 0.1$ (i.e., $f^{(4)}$ more than 3 σ away from $f_m^{(4)}$) would be required if the second companion was a main-sequence star with $m_2 \geq 0.1\ M_\odot$.

Instead, our results clearly suggest that the second companion is a $\sim 0.01\ M_\odot$ brown dwarf or giant planet. This is surprising since low-mass objects are not expected to be found in the cores of globular clusters. The reason is that low-mass objects have higher velocities in energy equipartition and are preferentially ejected from globular clusters as they evaporate in the tidal field of the Galaxy. Hence we do not expect to find very low mass stars or brown dwarfs in globular clusters, especially not near their cores. Recent *Hubble Space Telescope* (*HST*) observations of globular clusters (e.g., Paresce, De Marchi, & Romaniello 1995) also support this view by finding that stellar mass functions in clusters flatten or even drop for masses below $\sim 0.1\ M_\odot$. In addition, if the second companion of PSR B1620−26 is indeed of low mass, then the unusually high eccentricity of the inner binary pulsar cannot be explained by secular perturbations due to the second companion, since that would require a stellar-mass second companion (Rasio 1994). It would also preclude any possibility of an optical identification of the triple system. Bailyn et al. (1994) have searched deep optical images of M4 for an optical counterpart of the pulsar. They have identified a candidate that, if interpreted as a single object, could be a $0.45\ M_\odot$ main-sequence star within 0.″3 of the nominal pulsar position. However, it is possible that this object is in fact a blend of fainter stars not associated with the pulsar, or simply a chance superposition. Future observations of the region with *HST*, as well as improved ground-based astrometry, should help resolve the issue.

Low-mass stars and brown dwarfs could exist in dense globular cluster cores as binary companions to more massive stars. Dynamical interactions could then lead to an exchange, leaving the low-mass object in orbit around a neutron star. Indeed, Sigurdsson (1992) had discussed the possibility of finding planetary companions to pulsars in globular clusters even before the triple nature of PSR B1620−26 was established. A possible formation scenario for the triple system starts with an interaction between a neutron star–white dwarf binary and a main-sequence star with a large Jupiter-type planet or brown dwarf companion (cf. Sigurdsson 1993, 1995). As a result of this interaction, the white dwarf is ejected while the main-sequence star and its planet or brown dwarf companion remain in orbit around the neutron star. The main-sequence star, as it evolves and later expands as a red giant, would then transfer mass onto the neutron star, thus spinning it up and forming the millisecond pulsar in the triple configuration we see today. However, tidal dissipation during the mass transfer phase would effectively circularize the orbit of the binary, leaving a residual eccentricity $e_1 \lesssim 10^{-4}$ (Phinney 1992). Therefore this formation scenario leaves the much higher observed eccentricity ($e_1 \approx 0.03$) of the inner binary unexplained. It has been suggested that the eccentricity of the inner binary may have been induced during a dynamical interaction with another cluster star. The probability of disrupting the triple during such an interaction is only ~ 0.5 (Sigurdsson 1995). Based on the results of Rasio & Heggie (1995), however, we find that the observed eccentricity would require an encounter with a distance of closest approach of ~ 2.5 AU, considerably smaller than the size of the outer orbit and occurring on average once in $\sim 4 \times 10^8$ yr. For comparison, the lifetime of the triple system in the cluster is only about $\tau \sim (10^8\ \mathrm{yr})\rho_4^{-1}\sigma_5[a_2/(10\ \mathrm{AU})]^{-1} \sim 2 \times 10^7$ yr, where $\rho = 10^4\rho_4\ M_\odot\ \mathrm{pc}^{-3}$ is the density near the center of M4, $\sigma = 5\sigma_5$ km s^{-1} is the velocity dispersion, and a_2 is the size of the outer orbit (Rasio 1994). For one interaction that could have produced the eccentricity of the inner binary, we therefore expect ~ 20 interactions that could have disrupted the triple, each with probability ~ 0.5, leaving the probability of survival at $\sim 10^{-6}$. An additional problem is that the age of the millisecond pulsar in this scenario must be comparable to the age of the triple ($\sim 10^7$ yr), which requires the millisecond pulsar to be extremely young. This problem could be avoided if the triple was instead formed during an interaction involving a *preexisting* binary millisecond pulsar and another primordial binary (containing the present second companion and another star that was ejected during the interaction; see Rasio et al. 1995). The current eccentricity of the (inner) binary pulsar could then have been induced during the same interaction that formed the triple, although this would require some fine-tuning. More significantly, one would expect the more massive member of the other binary, rather than the low-mass object (Jupiter or brown dwarf), to be preferentially retained in the triple while the other was ejected.

Naturally, if the low-mass object (Jupiter or brown dwarf) was attached to a much more massive star, it is easier to understand how it was retained by the cluster and why it is now found close to the cluster core. In particular, in the first formation scenario discussed above, the main-

sequence star must have been fairly massive ($m \sim 1\ M_\odot$) to have evolved into a red giant after the triple was formed. Two-body relaxation in the cluster will tend to bring this main-sequence star (with its attached low-mass companion) down to the cluster core since it is more massive than the average object in the cluster. Confirmation of the existence of a $\sim 0.01\ M_\odot$ object in PSR B1620−26 would therefore provide further indication that many stars, even in globular clusters, could have very low mass companions or planets. This is especially important in light of recent discoveries of several $\sim 10^{-3}$ to $\sim 10^{-2}\ M_\odot$ objects around nearby stars (e.g., Mayor & Queloz 1995; Butler & Marcy 1996; Marcy & Butler 1996).

4. APPLICATION TO THE PSR B1257+12 PLANETARY SYSTEM

We now turn to the application of our method to the planetary system around the millisecond pulsar PSR B1257+12. This system contains three confirmed Earth-mass planets in quasi-circular orbits (Wolszczan & Frail 1992; Wolszczan 1994). The planets have masses of $0.015/\sin i_1\ M_\oplus$, $3.4/\sin i_2\ M_\oplus$, and $2.8/\sin i_3\ M_\oplus$, where i_1, i_2, and i_3 are the inclinations of the orbits with respect to the line of sight, and are at distances of 0.19, 0.36, and 0.47 AU, respectively, from the pulsar. In addition, the unusually large second and third frequency derivatives of the pulsar suggest the existence of a fourth, more distant and massive planet in the system (Wolszczan 1996).

4.1. *Analysis of the Frequency-Derivative Data*

The residual pulse frequency derivatives for PSR B1257+12 (after subtraction of a model for the inner three planets) are $\dot{f} = -8.6 \times 10^{-16}\ \mathrm{s}^{-2}$, $\ddot{f} = (-1.25 \pm 0.05) \times 10^{-25}\ \mathrm{s}^{-3}$, and $f^{(3)} = (1.1 \pm 0.3) \times 10^{-33}\ \mathrm{s}^{-4}$ (Wolszczan 1996) while the frequency $f = 160.8\ \mathrm{s}^{-1}$. The value of $\dot{f}$ has been corrected for the apparent acceleration due to the pulsar's transverse velocity (the so-called Shlovskii effect; see Camilo et al. 1994). The errors on f and $\dot{f}$, for the purposes of this discussion, are negligible. Note that the measurement of $f^{(3)}$ is only preliminary, but we assume here that the value quoted above (from Wolszczan 1996) is correct. Comparison with PSR B1855+09, which has a very similar pulse frequency, $f = 186\ \mathrm{s}^{-1}$, and first frequency derivative $\dot{f} = -6.2 \times 10^{-16}\ \mathrm{s}^{-2}$ (Kaspi et al. 1994), indicates that the observed $\dot{f}$ for PSR B1257+12 could well be entirely (or in large part) intrinsic rather than acceleration induced. The timing age for the pulsar, $\tau = -\frac{1}{2} f/\dot{f} \sim 3 \times 10^9$ yr, is entirely consistent with that expected for a millisecond pulsar. Therefore we will treat $\dot{f}_{\rm acc}$ essentially as a free parameter in our analysis. The observed $\ddot{f}$, on the other hand, is 2 orders of magnitude larger than for PSR B1855+09, which has $\ddot{f} \leq 2.0 \times 10^{-27}\ \mathrm{s}^{-2}$. Thus the observed $\ddot{f}$ is almost certainly due to the presence of another planet rather than to intrinsic timing noise in the pulsar.

With three frequency derivatives measured, we can use the method of § 2.3 to model the system. Given the nearly circular orbits of the three inner planets, it is natural to assume that the orbit of the fourth planet also has a low eccentricity. In addition, it is easy to show that dynamical interactions with passing stars in the Galaxy are not likely to produce any significant perturbations of the system (which could otherwise increase the eccentricity of an outer planet's orbit; see Heggie & Rasio 1996).

Since the value of $\dot{f}_{\rm acc}$ is uncertain, we explore a wide range, $0.01 < \dot{f}_{\rm acc}/\dot{f}_{\rm obs} < 1$. Note that, for a circular orbit, $\dot{f}_{\rm acc}$ and $f^{(3)}$ must have opposite signs (cf. eqs. [19] and [21]). Hence $\dot{f}_{\rm acc}$ cannot be positive. For each value of $\dot{f}_{\rm acc}$, we calculate the mass and semimajor axis of the fourth planet by using equations (25), (28), and (30). We illustrate the results in Figure 10. We find that the mass of the fourth planet varies significantly, from $\sim 0.08\ M_\oplus$ (for $\dot{f}_{\rm acc} = 0.01\dot{f}_{\rm obs}$) to $\sim 100\ M_\oplus$ (for $\dot{f}_{\rm acc} = \dot{f}_{\rm obs}$). The simplest interpretation of the present best-fit values of the frequency derivatives, assuming $\dot{f}_{\rm acc} = \dot{f}_{\rm obs}$, implies a mass of about $100/\sin i_4\ M_\oplus$ (i.e., comparable to Saturn's mass) for the fourth planet, at a distance of about 38 AU (i.e., comparable to Pluto's distance from the Sun), and with a period of about 170 yr in a circular, coplanar orbit (Wolszczan 1996). However, if $\dot{f}_{\rm acc} \neq \dot{f}_{\rm obs}$, then the fourth planet can have a wide range of masses. In particular, it can have a mass comparable to that of Mars (at a distance of 9 AU), Uranus (at a distance of 25 AU), or Neptune (at a distance of 26 AU), for $\dot{f}_{\rm acc} = 0.015\dot{f}_{\rm obs}$, $0.30\dot{f}_{\rm obs}$, or $0.34\dot{f}_{\rm obs}$, respectively.

4.2. *Discussion*

In this system, the perturbations of the inner planets produced by the fourth planet are probably far too small to be detected. This is in contrast to the mutual perturbations of the inner planets themselves, which are important and have been detected (Rasio et al. 1992; Wolszczan 1994). Using equations (33)–(36), we predict $\dot{e} \sim 10^{-17}\ \mathrm{s}^{-1}$ and $\dot{\omega} \sim 10^{-7}$

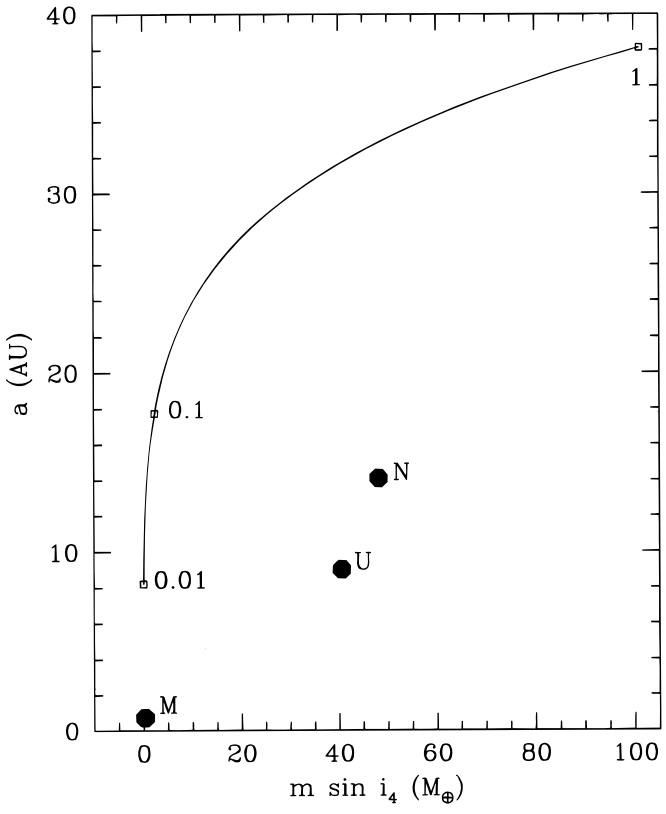

FIG. 10.—Mass and semimajor axis of the possible outer planet in the PSR B1257+12 planetary system for $\dot{f}_{\rm acc}$ in the range $(0.01\text{–}1.0)\dot{f}_{\rm obs}$. The present best-fit values of the frequency derivatives with $\dot{f}_{\rm acc} = \dot{f}_{\rm obs}$ imply the presence of a planet with mass $\approx 100/\sin i_4\ M_\oplus$, at a distance of ≈ 38 AU. The marked points on the curve indicate the values of $\dot{f}_{\rm acc}/\dot{f}_{\rm obs}$. The points labeled M, U, and N indicate configurations with the same mass and radius ratios (in this system) as those of Mars, Uranus, and Neptune (in the solar system), respectively.

deg yr^{-1} for the orbit of the third planet, assuming that all orbits are coplanar and that the mass of the fourth planet is 100 $M_\oplus$. The perturbations for the two innermost planets are even smaller. Hence the existence of the fourth planet is likely to be confirmed only through further measurements of pulse frequency derivatives.

It has been pointed out that the masses and radii of the three inner planets in PSR B1257+12 are in the same ratios as the masses and radii of the corresponding first three planets in the solar system (Mazeh & Goldman 1995). This might perhaps be indicative of a global underlying formation mechanism for the two systems.

Although the fourth planet could have the same mass (normalized to the mass of the third planet) as Mars, Uranus, or Neptune (normalized to the mass of the Earth), the ratio of radii in each case would be much larger than the corresponding ratio for the solar system (cf. Fig. 10). Thus this system does not seem to maintain its regularity with the solar system, since the mass and radius ratios of the fourth planet would not simultaneously match those of any planet in the solar system. This is true for the entire range of values of $\dot{f}_{\rm acc}$ considered above.

We are very grateful to Z. Arzoumanian, S. E. Thorsett, and A. Wolszczan for many useful discussions and for communicating results of observations in progress. We also thank C. Bailyn and S. Sigurdsson for helpful comments. F. A. R. is supported by an Alfred P. Sloan Research Fellowship.

APPENDIX

GEOMETRY OF THE TRIPLE CONFIGURATION

The orbit of the inner binary and the orbit of the second companion in general do not lie in the same plane. The inclinations of the two planes with respect to the line of sight are given by i_1 and i_2. To specify the plane of an orbit completely, one needs the inclination angle together with another azimuthal angle α (which lies between 0 and 2π). Since the reference axis for α is arbitrary, we can take it to lie in the plane of one of the orbits, so that α is the difference between the azimuthal angles of the two planes. In random Monte Carlo trials, α is then taken to be uniformly distributed between 0 and 2π.

In order to determine θ_2 and ϕ_2 using the other angles, we need to change coordinates between two reference frames. The first frame has its origin at the center of mass of the inner binary, with the x-axis in the plane of the orbit of the second companion, the y-axis passing through the pericenter of the orbit, and the z-axis perpendicular to the plane of the orbit, so that the motion of second companion is counterclockwise around the z-axis. We shall refer to the coordinates of the second companion in this frame as (x_c', y_c', z_c'). Then $x_c' = -r_{12} \sin \lambda_2$, $y_c' = r_{12} \cos \lambda_2$, and $z_c' = 0$.

The second frame similarly has its origin at the center of mass of the inner binary, with the x-axis in the plane of the orbit of the inner binary, the y-axis passing through the pericenter of the orbit, and the z-axis perpendicular to the plane of the orbit, so that the motion of pulsar is counterclockwise around the z-axis. We wish to find the coordinates (x_c'', y_c'', z_c'') of the second companion in this frame. We can then calculate θ_2 and ϕ_2 using the formulae $\theta_2 = \cos^{-1}(z_c''/r_{12})$ and $\phi_2 = \tan^{-1}(-x_c''/y_c'')$, keeping in mind that for $y_c'' < 0$ we must add 180° to ϕ_2 in order to obtain the correct quadrant.

In order to obtain (x_c'', y_c'', z_c'') from (x_c', y_c', z_c'), we rotate the first frame to the second frame, using the standard Euler angles formalism (see, e.g., Goldstein 1980). In this formalism, any arbitrary rotation of an object is represented as a sequence of three consecutive rotations—first about the z-axis by an angle ϕ, then about the new x-axis by an angle θ, and finally again about the new z-axis by an angle ψ.

In order to use this formalism, we use an intermediate frame of reference that is fixed in space, with its origin at the center of mass of the inner binary, the y-axis along the line of sight, the x-axis in the plane of the orbit of the second companion, and the z-axis such that the motion of the second companion is counterclockwise about the z-axis. The first frame described above can be obtained from this fixed frame by rotating it through the Euler angles 0, i_2, and $\omega_2 - 90°$, respectively. Similarly, the second frame can be obtained from the fixed frame by rotating it through the angle α about the y-axis and then rotating it through the Euler angles 0, i_1, and $\omega_1 - 90°$, respectively. The sequence of Euler angle rotations is represented as a matrix $\mathbf{A}(\phi, \theta, \psi)$. We obtain the coordinates (x_c'', y_c'', z_c'') from (x_c', y_c', z_c') by multiplying first by the inverse matrix $\mathbf{A}^{-1}(0, i_2, \omega_2 - 90°)$, then multiplying by the matrix for rotation about the y-axis $\mathbf{B}(\alpha)$, and then multiplying by the matrix $\mathbf{A}(0, i_1, \omega_1 - 90°)$. The matrices are given by

$$\mathbf{A}(\phi, \theta, \psi) = \begin{pmatrix} \cos\psi\cos\phi - \cos\theta\sin\phi\sin\psi & \cos\psi\sin\phi + \cos\theta\cos\phi\sin\psi & \sin\psi\sin\theta \\ -\sin\psi\cos\phi - \cos\theta\sin\phi\cos\psi & -\sin\psi\sin\phi + \cos\theta\cos\phi\cos\psi & \cos\psi\sin\theta \\ \sin\theta\sin\phi & -\sin\theta\cos\phi & \cos\theta \end{pmatrix},$$

$$\mathbf{B}(\alpha) = \begin{pmatrix} \cos\alpha & 0 & -\sin\alpha \\ 0 & 1 & 0 \\ \sin\alpha & 0 & \cos\alpha \end{pmatrix},$$

REFERENCES

Arzoumanian, Z., Joshi, K. J., Rasio, F. A., & Thorsett, S. E. 1996, in IAU Colloq. 160, Pulsars: Problems and Progress, ed. S. Johnston, M. A. Walker, & M. Bailes (ASP Conf. Proc. 105) (San Francisco: ASP), 525
Arzoumanian, Z., Nice, D. J., Taylor, J. H., & Thorsett, S. E. 1994, ApJ, 422, 621
Arzoumanian, Z., & Thorsett, S. E. 1997, in preparation
Backer, D. C. 1993, in ASP Conf. Proc. 36, Planets around Pulsars, ed. J. A. Phillips, S. E. Thorsett, & S. R. Kulkarni (San Francisco: ASP), 11
Backer, D. C., Foster, R. S., & Sallmen, S. 1993, Nature, 365, 817
Bailyn, C. D., Rubinstein, E. P., Girard, T. M., Dinescu, D. I., Rasio, F. A., & Yanny, B. 1994, ApJ, 433, L89

Butler, P. R., & Marcy, G. W. 1996, ApJ, 464, L153
Camilo, F., Thorsett, S. E., & Kulkarni, S. R. 1994, ApJ, 421, L15
Eggleton, P., & Kiseleva, L. 1995, ApJ, 455, 640
Goldstein, H. 1980, Classical Mechanics (2d ed.; Reading, MA: Addison-Wesley)
Heggie, D. C. 1975, MNRAS, 173, 729
Heggie, D. C., & Rasio, F. A. 1996, MNRAS, 282, 1064
Kaspi, V. M., Taylor, J. H., & Ryba, M. F. 1994, ApJ, 428, 713
Lorimer, D. R., Lyne, A. G., Festin, L., & Nicastro, L. 1995, Nature, 376, 393
Lyne, A. G., Biggs, J. D., Brinklow, A., Ashworth, M., & McKenna, J. 1988, Nature, 332, 45
Marcy, G. W., & Butler, P. R. 1996, ApJ, 464, L147
Mayor, M., & Queloz, D. 1995, Nature, 378, 355
Mazeh, T., & Goldman, I. 1995, PASP, 107, 250
McKenna, J., & Lyne, A. G. 1988, Nature, 336, 226 (erratum 336, 698)
Michel, F. C. 1994, ApJ, 432, 239
Paresce, F., De Marchi, G., & Romaniello, M. 1995, ApJ, 440, 216
Phinney, E. S. 1992, Phil. Trans. R. Soc. London A, 341, 39
Phinney, E. S., & Kulkarni, S. R. 1994, ARA&A, 32, 591
Press, W. H., Teukolsky, S. A., Vetterling, W. T., & Flannery, B. P. 1992, Numerical Recipes in C (2d ed.; New York: Cambridge Univ. Press)
Rasio, F. A. 1994, ApJ, 427, L107
Rasio, F. A., & Heggie, D. C. 1995, ApJ, 445, L133
Rasio, F. A., McMillan, S., & Hut, P. 1995, ApJ, 438, L33
Rasio, F. A., Nicholson, P. D., Shapiro, S. L., & Teukolsky, S. A. 1992, Nature, 355, 325
Sigurdsson, S. 1992, ApJ, 399, L95
———. 1993, ApJ, 415, L43
———. 1995, ApJ, 452, 323
Thorsett, S. E., Arzoumanian, Z., & Taylor, J. H. 1993, ApJ, 412, L33
Wolszczan, A. 1994, Science, 264, 538
———. 1996, in IAU Colloq. 160, Pulsars: Problems and Progress, ed. S. Johnston, M. A. Walker, & M. Bailes (ASP Conf. Proc. 105) (San Francisco: ASP), 91
Wolszczan, A., & Frail, D. A. 1992, Nature, 355, 145
Wolszczan, A., Kulkarni, S. R., Middleditch, J., Backer, D. C., Fruchter, A. S., & Dewey, R. J. 1989, Nature, 337, 531

THE ASTROPHYSICAL JOURNAL, 488:901, 1997 October 20

ERRATUM

In the paper "Distant Companions and Planets around Millisecond Pulsars" by Kriten J. Joshi and Frederic A. Rasio (ApJ, 479, 948 [1997]), the following corrections should be made:

In equations (16), (17), and (18), the factor $\sin \lambda_1$ in the denominator should be changed to $\sin (\lambda_1 + \omega_1)$, and the expression in equation (18) should have a negative sign. The revised equations are as follows:

$$h = -\left[\frac{\dot{f}cA^2}{f \sin i_2 \sin (\lambda_1 + \omega_1)\dot{\lambda}_1^2}\right], \tag{16}$$

$$k = -\left[\frac{\dot{f}c}{f \sin i_2 \sin (\lambda_1 + \omega_1)}\right]^3 \left(\frac{A^2}{\dot{\lambda}_1^4}\right), \tag{17}$$

$$m_2 \sin i_2 \approx \frac{-\dot{f}c}{f \sin (\lambda_1 + \omega_1)} \left(\frac{m_1^2 A^2}{G\dot{\lambda}_1^4}\right)^{1/3}. \tag{18}$$

These corrections are only typographical in nature, and none of the results or conclusions of the paper are affected.

In addition, in equation (32) the sign of the third term $(2.2/(1 + q_{out}^{1/3}))$ should be changed to negative. This typographical error is also in the original reference (Eggleton & Kiseleva 1995) from which the equation was taken. This does not affect the ultimate lower bound for the mass m_2 since a stronger constraint is imposed by the lack of any observed periodicity in the timing residuals.